

The ephrin receptor tyrosine kinase A2 is a cellular receptor for Kaposi's sarcoma-associated herpesvirus

Alexander S Hahn^{1,8}, Johanna K Kaufmann^{1,8,9}, Effi Wies^{1,8,9}, Elisabeth Naschberger², Julia Panteleev-Ivlev¹, Katharina Schmidt¹, Angela Holzer¹, Martin Schmidt¹, Jin Chen^{3,4}, Simone König⁵, Armin Ensser¹, Jinjong Myoung⁶, Norbert H Brockmeyer⁷, Michael Stürzl², Bernhard Fleckenstein¹ & Frank Neipel¹

Kaposi's sarcoma-associated herpesvirus (KSHV) is the causative agent of Kaposi's sarcoma¹, a highly vascularized tumor originating from lymphatic endothelial cells, and of at least two different B cell malignancies^{2,3}. A dimeric complex formed by the envelope glycoproteins H and L (gH-gL) is required for entry of herpesviruses into host cells⁴. We show that the ephrin receptor tyrosine kinase A2 (EphA2) is a cellular receptor for KSHV gH-gL. EphA2 co-precipitated with both gH-gL and KSHV virions. Infection of human epithelial cells with a GFP-expressing recombinant KSHV strain, as measured by FACS analysis, was increased upon overexpression of EphA2. Antibodies against EphA2 and siRNAs directed against EphA2 inhibited infection of endothelial cells. Pretreatment of KSHV with soluble EphA2 resulted in inhibition of KSHV infection by up to 90%. This marked reduction of KSHV infection was seen with all the different epithelial and endothelial cells used in this study. Similarly, pretreating epithelial or endothelial cells with the soluble EphA2 ligand ephrinA4 impaired KSHV infection. Deletion of the gene encoding EphA2 essentially abolished KSHV infection of mouse endothelial cells. Binding of gH-gL to EphA2 triggered EphA2 phosphorylation and endocytosis, a major pathway of KSHV entry^{5,6}. Quantitative RT-PCR and *in situ* histochemistry revealed a close correlation between KSHV infection and EphA2 expression both in cultured cells derived from human Kaposi's sarcoma lesions or unaffected human lymphatic endothelium, and *in situ* in Kaposi's sarcoma specimens, respectively. Taken together, our results identify EphA2, a tyrosine kinase with known functions in neovascularization and oncogenesis, as an entry receptor for KSHV.

Herpesvirus entry involves several viral glycoproteins and cellular receptors^{4,7}. KSHV uses cell surface heparan sulfate⁸⁻¹¹ or DC-SIGN¹² for attachment. Subsequently, KSHV binding to integrins

activates several downstream effectors^{13,14} followed by endocytosis^{5,6}. The cysteine transporter xCT was identified as a fusion receptor for KSHV¹⁵. However, the viral glycoproteins responsible for interactions with xCT have not been identified. In the case of KSHV, gB and gH-gL seem to comprise the minimal fusion machinery¹⁶. We previously reported that the gH-gL complex binds an unknown receptor on the heparan sulfate-negative mouse fibroblast cell line sog9 (ref. 11).

To identify this putative KSHV receptor, we surface-biotinylated sog9 cells¹⁷, lysed them and subjected the lysate to immunoprecipitation with a soluble variant of gH lacking the transmembrane and intracellular part fused to the Fc fragment of human IgG (gHΔTM-Fc) that was co-expressed in complex with gL (gHΔTM-Fc/gL) (Fig. 1a). We identified by mass spectrometry a membrane protein of ~110 kDa that specifically interacted with this glycoprotein complex as EphA2 (Supplementary Table 1). Immunoprecipitation with gHΔTM-Fc/gL from 293T human embryonic kidney cells expressing Myc- and His-tagged EphA2 lacking the intracellular domain (EphA2ΔICMycHis) confirmed this interaction (Fig. 1b). Soluble EphA2 also bound to 293T cells expressing KSHV gH-gL (Supplementary Fig. 1). However, only KSHV gH-gL precipitated EphA2 whereas gH-gL from the related rhesus monkey rhadinovirus (RRV) did not (Fig. 1c). Co-sedimentation experiments were performed using KSHV virions concentrated from the supernatant of the KSHV-positive primary effusion lymphoma (PEL) cell line BC3 to further prove that EphA2 is associated with gH-gL in the virion envelope. The recombinantly expressed hemagglutinin-tagged ectodomain of EphA2 (EphA2-HA) was incubated with precleared supernatant from BC3 cells that were either induced to produce KSHV virions or left uninduced (mock). KSHV virions were then pelleted by centrifugation and subjected to western blot analysis. The virion envelope protein gpK8.1 did not bind directly to EphA2 (data not shown). Due to alternative splicing and glycosylation, different forms of the viral envelope glycoprotein gpK8.1 are expressed in cells lytically infected with KSHV. The predominant

¹Virologisches Institut, Universitätsklinikum Erlangen, Erlangen, Germany. ²Abteilung für Molekulare und Experimentelle Chirurgie, Universitätsklinikum Erlangen, Erlangen, Germany. ³Departments of Medicine, Cancer Biology, Cell and Developmental Biology, Vanderbilt-Ingram Cancer Center, Vanderbilt University, Nashville, Tennessee, USA. ⁴Veterans Affairs Medical Center, Tennessee Valley Healthcare System, Nashville, Tennessee, USA. ⁵Integrated Functional Genomics, Interdisciplinary Center of Clinical Research, University of Münster, Münster, Germany. ⁶Novartis Institutes for Biomedical Research, Emeryville, California, USA. ⁷Department for Dermatology, St. Josef-Hospital, Bochum, Germany. ⁸Present addresses: New England Primate Research Center, Harvard Medical School, Southborough, Massachusetts, USA (A.H. and E.W.); German Cancer Research Center, Heidelberg, Germany (J.K.K.). ⁹These authors contributed equally to this work. Correspondence should be addressed to F.N. (frank.neipel@viro.med.uni-erlangen.de).

Received 28 November 2011; accepted 17 April 2012; published online 27 May 2012; doi:10.1038/nm.2805

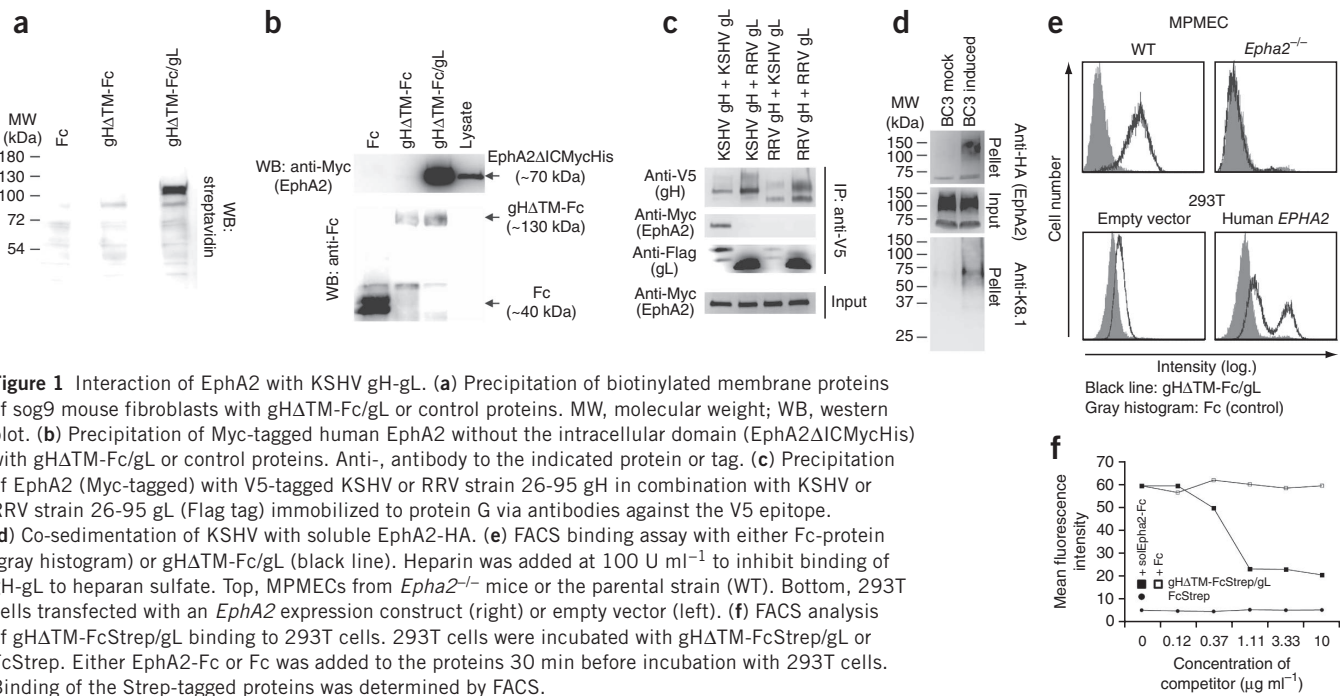


Figure 1 Interaction of EphA2 with KSHV gH-gL. **(a)** Precipitation of biotinylated membrane proteins of sog9 mouse fibroblasts with gH Δ TM-Fc/gL or control proteins. MW, molecular weight; WB, western blot. **(b)** Precipitation of Myc-tagged human EphA2 without the intracellular domain (EphA2 Δ ICMycHis) with gH Δ TM-Fc/gL or control proteins. Anti-, antibody to the indicated protein or tag. **(c)** Precipitation of EphA2 (Myc-tagged) with V5-tagged KSHV or RRV strain 26-95 gH in combination with KSHV or RRV strain 26-95 gL (Flag tag) immobilized to protein G via antibodies against the V5 epitope. **(d)** Co-sedimentation of KSHV with soluble EphA2-HA. **(e)** FACS binding assay with either Fc-protein (gray histogram) or gH Δ TM-Fc/gL (black line). Heparin was added at 100 U ml⁻¹ to inhibit binding of gH-gL to heparan sulfate. Top, MPMECs from *Epha2*^{-/-} mice or the parental strain (WT). Bottom, 293T cells transfected with an *Epha2* expression construct (right) or empty vector (left). **(f)** FACS analysis of gH Δ TM-FcStrep/gL binding to 293T cells. 293T cells were incubated with gH Δ TM-FcStrep/gL or FcStrep. Either EphA2-Fc or Fc was added to the proteins 30 min before incubation with 293T cells. Binding of the Strep-tagged proteins was determined by FACS.

variant of gpK8.1 that is present in cellular membranes migrates with an apparent molecular weight of 35–37 kDa. In contrast, a protein of 68–72 kDa is selectively incorporated into the virion envelope¹⁸. Co-sedimentation of EphA2-HA with a gpK8.1 protein of 68–72 kDa¹⁸ and not the cell-membrane variant of 35 kDa demonstrated association of EphA2 with virions (**Fig. 1d**). Having shown that soluble EphA2 is able to bind both isolated gH-gL (**Fig. 1b,c** and **Supplementary Fig. 1**) and KSHV (**Fig. 1d**), we next examined whether gH-gL is able to bind membrane-bound EphA2. We added heparin to the recombinantly expressed gH-gL glycoprotein complex to inhibit binding of gH-gL to heparan sulfate¹¹. We incubated mouse pulmonary microvascular endothelial cells (MPMECs) from either an *Epha2*-knockout mouse or the parental mouse strain (WT) with gH Δ TM-Fc/gL. Binding of gH Δ TM-Fc/gL to WT MPMECs in the presence of heparin was clearly detectable, whereas MPMECs from an *Epha2*-knockout mouse¹⁹ did not bind gH Δ TM-Fc/gL (**Fig. 1e**). Overexpression of EphA2 greatly increased binding of gH Δ TM-Fc/gL to 293T cells (**Fig. 1e**), whereas competition with soluble EphA2-Fc reduced binding of gH Δ TM-Fc/gL to these cells (**Fig. 1f**). This finding is particularly noteworthy because heparin was not used here (**Fig. 1f**), and both gH alone and the gH-gL complex bind cell-surface heparan sulfates with high affinity¹¹.

The inhibition of the interaction of gH Δ TM-Fc/gL with the cell surface by soluble EphA2 (**Fig. 1f**) raised the question of whether soluble EphA2 is able to influence KSHV infection. To address this question we used the recombinant KSHV strain rKSHV.219 (ref. 20). rKSHV.219 carries the gene encoding GFP under the control of a cellular constitutive promoter. This allows the detection of KSHV-infected cells by fluorescence microscopy or FACS analysis. When we incubated rKSHV.219 with EphA2-Fc before infection of human lymphatic endothelial cells (LECs), primary Kaposi's sarcoma spindle cells (M7/2 (ref. 21)) and two established Kaposi's sarcoma cell lines (KSImm²² and SLK²³), EphA2-Fc inhibited KSHV infection in a dose-dependent manner by up to 97% (**Fig. 2a** and **Supplementary Fig. 2**). Half-maximal inhibition of KSHV infection was achieved at a concentration of

<0.2 μ g ml⁻¹, which corresponds to approximately 1 nM of dimeric EphA2-Fc (**Fig. 2a**). A recombinant herpesvirus saimiri serving as a control was unaffected by EphA2-Fc (**Supplementary Fig. 3a**).

In addition to blocking the EphA2 binding site(s) on KSHV virions with soluble EphA2 (**Fig. 2a** and **Supplementary Fig. 2**), we also blocked EphA2 on primary human umbilical vein endothelial cells (HUVECs) and primary human LECs with a polyclonal antibody against EphA2 before KSHV infection, resulting in a significant reduction of KSHV infection (**Fig. 2b**, $P < 0.001$). In contrast to KSHV infection, infection with herpesvirus saimiri was not inhibited by EphA2-specific antibody (**Supplementary Fig. 3b**). Overexpression of EphA2 in two human epithelial cell lines (293T and H1299) resulted in increased KSHV infection (**Supplementary Fig. 4**). We confirmed the relevance of EphA2 in infection of endothelial cells by RNAi (**Fig. 2c**); siRNA against EphA2 specifically reduced infection of LECs by approximately 70% (nonsense siRNA siNon versus siEphA2, Student's t test, $P < 0.05$). Silencing of EphA2 was verified by FACS analysis (**Supplementary Fig. 5**).

We performed additional control experiments using (i) soluble EphA2 without the Fc tag, (ii) the closely related protein EphA5, (iii) the soluble EphA2 ligand ephrinA4-Fc, which induces EphA2 signaling, (iv) preincubation of the cells, rather than KSHV, with EphA2 and (v) soluble integrins and heparin for comparison (**Fig. 2d,e**). The GFP-expressing rKSHV.219 was used again. We determined infection rates by FACS analysis for GFP expression and by quantitative real time-PCR (qRT-PCR) for the KSHV latency-associated nuclear antigen-1 (LANA-1) transcript. Preincubation of KSHV with EphA2-Fc or monomeric EphA2, in contrast to preincubation with the closely related EphA5, resulted in a significant reduction of infection that was comparable to the inhibitory effect of the virion-attachment inhibitor heparin, as did preincubation of the cells with ephrinA4-Fc (**Fig. 2d**). Surprisingly, in contrast to data from other groups^{5–7,14}, preincubation of KSHV with integrin $\alpha_3\beta_1$ or integrin $\alpha_v\beta_3$ did not inhibit KSHV infection, and pretreatment of SLK cells with antibody LM609, specific for integrin $\alpha_v\beta_3$, had only a very moderate effect

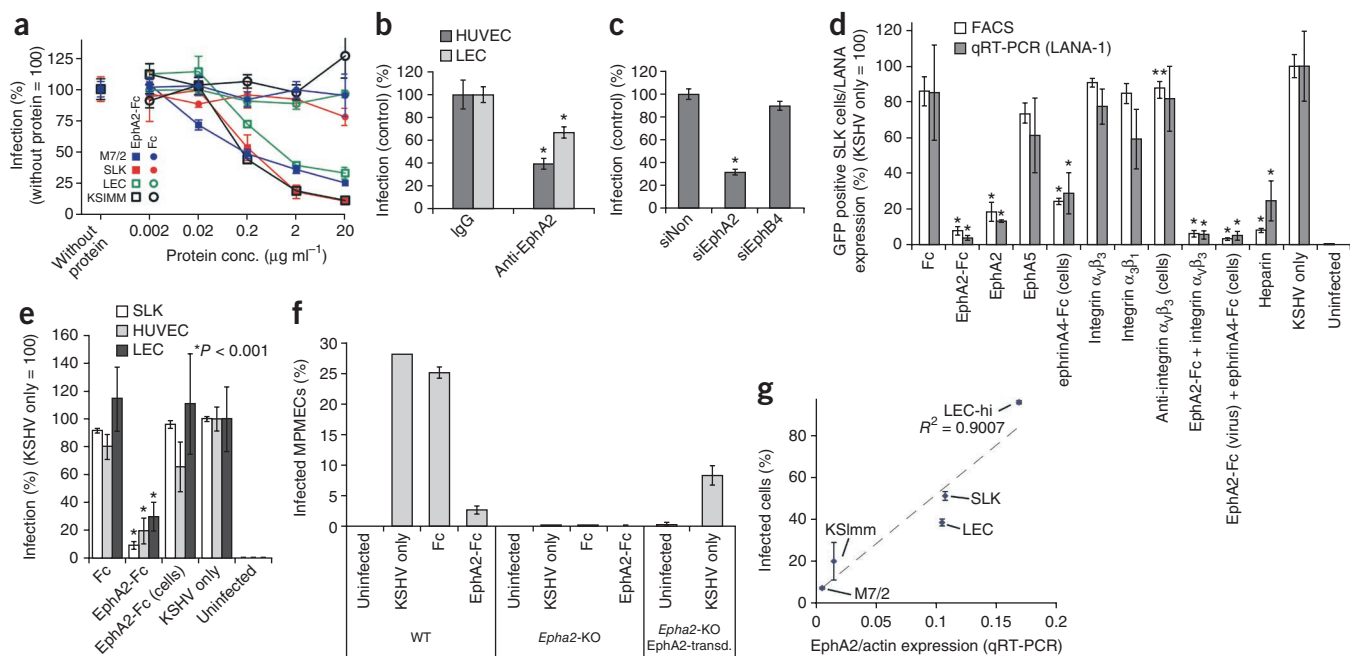


Figure 2 Analysis of KSHV susceptibility and EphA2 expression in cell culture. **(a)** Dose-dependent inhibition of KSHV infection by soluble EphA2. Infection of LECs, SLK cells, KSIImm cells and M7/2 cells. rKSHV.219 was preincubated with EphA2-Fc or Fc. Infection rate without protein was set to 100% (SLK and KSIImm $n = 6$, LEC and M7/2 $n = 3$, error bars represent s.d.). **(b)** Inhibition of KSHV infection by antibodies against EphA2. HUVECs and LECs were incubated with antibody to EphA2 or rabbit IgG and infected with rKSHV.219. Relative infection rates are shown ($n = 7$, error bars represent s.e.m.; $*P < 0.001$). **(c)** Infection of LECs after EphA2 knockdown. siNon was set to 100% relative infection ($n = 4$, error bars represent s.e.m.; $*P < 0.001$). **(d)** rKSHV.219 or, where indicated, the SLK target cells were pre-incubated with the indicated reagents at $2 \mu\text{g ml}^{-1}$ (integrins and anti-integrin $\alpha_v\beta_3$ at $10 \mu\text{g ml}^{-1}$; heparin at 166 IU ml^{-1}). Infection was determined by both FACS and qRT-PCR. KSHV only was set to 100% (FACS $n = 6$, qRT-PCR $n = 3$, error bars represent s.d.). Asterisks indicate statistically significant differences compared to KSHV only ($*P < 0.001$; $**P < 0.01$). **(e)** Infection of endothelial cells. Either the viral inoculum or the cells were preincubated with EphA2-Fc ($2 \mu\text{g ml}^{-1}$) or Fc (KSHV only = 100%, $n = 3$, error bars represent s.d.). Asterisks indicate statistically significant differences compared to KSHV only ($P < 0.001$). **(f)** Infection of MPMECs from either WT or an *Epha2*-knockout (KO) mouse or *Epha2*-knockout cells transduced with a mouse EphA2 cDNA as a control. Where indicated, KSHV was preincubated with EphA2-Fc or control protein ($2 \mu\text{g ml}^{-1}$, $n = 3$, error bars represent s.d.). **(g)** Correlation of EphA2 mRNA expression as determined by qRT-PCR and KSHV infection in human primary cells and cell lines ($R^2 =$ square correlation coefficient; SLK and KSIImm $n = 6$, otherwise $n = 3$).

(Fig. 2d). The discrepancy between these results and previously published work^{5–7,14} may reflect cell-specific usage of integrins by KSHV, and the role of integrins in the infection of endothelial cells and cells derived from Kaposi's sarcoma has not been examined so far. In summary, these data indicated that the observed inhibition of KSHV infection is specific for EphA2. However, it remained to be shown that this inhibitory effect is mediated by the interaction of EphA2-Fc with the KSHV virion and not the cell. Thus, we incubated either KSHV or the cells with EphA2-Fc 30 min prior to infection. We used soluble Fc as a control. Compared to both Fc pretreatment or the buffer control (KSHV only), only pretreatment of the viral inoculum with EphA2-Fc at $2 \mu\text{g ml}^{-1}$ resulted in a statistically significant reduction in KSHV infection (Fig. 2e). In contrast to the EphA2 ligand ephrinA4-Fc (Fig. 2d), soluble EphA2-Fc did not result in reduced infection when added to the cells (Fig. 2e). This shows that inhibition of infection by EphA2 requires the interaction of EphA2 with the KSHV virion.

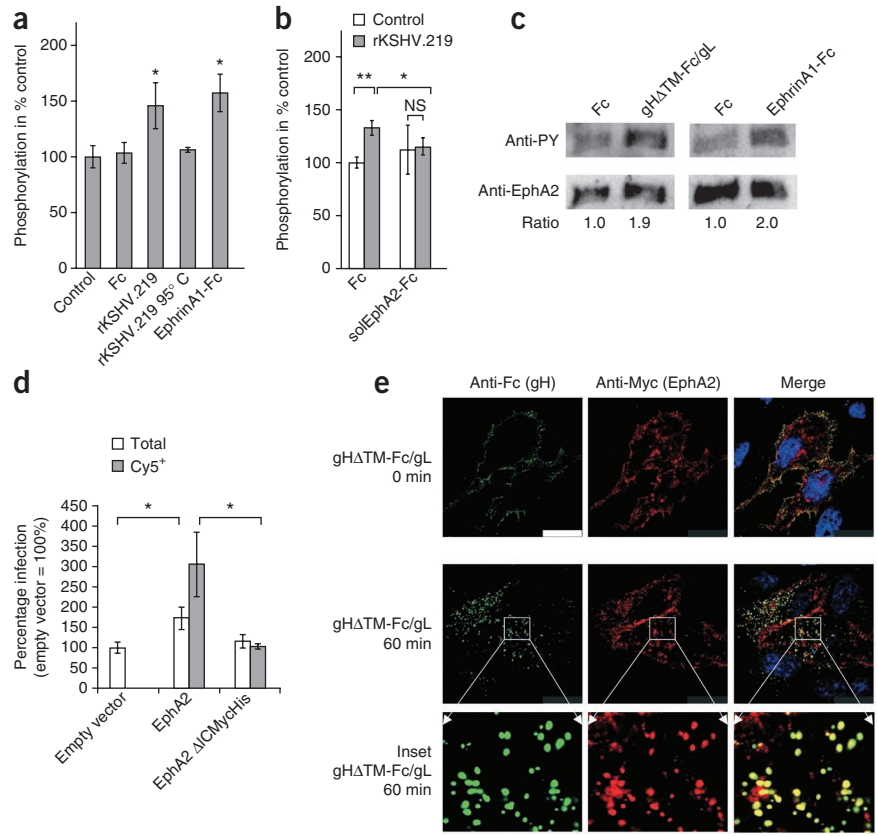
Infection of MPMECs with rKSHV.219 resulted in 25% infected cells at 3 d after infection. Preincubation of the virus with EphA2-Fc reduced infection by about 90% (Fig. 2f). MPMECs from an *Epha2*-knockout mouse were almost completely resistant to KSHV infection (Fig. 2f). When we reconstituted EphA2 expression in these knockout cells by a retroviral expression vector¹⁹, MPMECs from the *Epha2*^{-/-} mouse regained permissiveness (Fig. 2f).

Although many cell lines can be infected by KSHV, permissiveness for KSHV entry varies as reflected by the percentage of cells infected

using a constant MOI²⁴, as does expression of EphA2. We measured EphA2 mRNA expression levels by qRT-PCR in ten different types of primary human cells and human cell lines. EphA2-Fc ($2 \mu\text{g ml}^{-1}$) diminished KSHV infection by at least 50% in all cell lines examined (Supplementary Fig. 6). Plotting EphA2 mRNA expression against the infection rate revealed a linear correlation (Pearson's $r = 0.95$, $P = 0.014$) for cells of lymphatic endothelial origin (Fig. 2g). Notably, the permissiveness of two different batches of LECs varied about twofold (LEC and LEC-hi), which was reflected by the corresponding EphA2 expression.

To assess the effect of KSHV on EphA2 activation, we incubated 293T cells with concentrated supernatants either from 293 cells producing recombinant KSHV strain rKSHV.219 or uninfected control cells. EphrinA1-Fc was used as a positive control. Both rKSHV.219 and the natural EphA2 ligand ephrinA1 recombinantly expressed in fusion to the Fc (ephrinA1-Fc) increased EphA2 phosphorylation (Fig. 3a and Supplementary Fig. 7). EphA2 phosphorylation was reverted when KSHV was preincubated with EphA2-Fc (Fig. 3b). Next, we stimulated cellular EphA2 with gHΔTM-Fc/gL. Crosslinking of gHΔTM-Fc/gL through an Fc-specific antibody was required for activation of EphA2 (data not shown), mimicking higher-order clustering of envelope glycoproteins. Treatment of cells with cross-linked gHΔTM-Fc/gL or ephrinA1-Fc resulted in a marked increase in EphA2 phosphorylation, as detected by western blot (Fig. 3c). To determine whether these effects are of biological importance for KSHV entry, we transiently overexpressed either full-length EphA2 or

Figure 3 Phosphorylation and endocytosis of EphA2 in response to KSHV and gH-gL. (a) Phosphorylation of EphA2 as determined by ELISA after stimulation with KSHV. rKSHV.219 ($n = 5$), heat-denatured rKSHV.219 ($n = 2$), a control preparation with supernatant from KSHV-uninfected cells ($n = 5$) or Fc ($5 \mu\text{g ml}^{-1}$, $n = 5$). EphrinA1-Fc ($5 \mu\text{g ml}^{-1}$) served as a positive control ($n = 5$). The KSHV-negative control preparation was set to 100% (error bars represent s.d., $*P < 0.005$). (b) Inhibition of EphA2 phosphorylation in response to KSHV by soluble EphA2. 293T cells were stimulated with concentrated rKSHV.219 or control as in a. Fc or EphA2-Fc were added to $5 \mu\text{g ml}^{-1}$ 30 min before incubation with the cells. EphA2 phosphorylation was determined by ELISA (control preparation with Fc-protein = 100%; $n = 3$, error bars represent s.d., $*P < 0.05$, $**P < 0.005$; NS, not significant). (c) EphA2 phosphorylation as determined by western blotting after stimulation with preclustered gH Δ TM-Fc/gL or ephrinA1-Fc as a positive control. (d) Infection of 293T cells transfected with empty vector, an expression plasmid for EphA2 or EphA2 Δ IC. KSHV infection (GFP) and the transfected proteins (Cy5 fluorescence) were analyzed by FACS. Open bars represent rKSHV.219 infection in the total population; gray bars within the population of cells staining positive for the transfected constructs. Empty-vector-transfected cells were set to 100%. ($n = 3$, error bars represent s.d., $*P < 0.05$). (e) Immunofluorescence analysis of EphA2 and gH Δ TM-Fc/gL localization. gH Δ TM-Fc/gL was crosslinked for 30 min with Alexa 488-conjugated antibody to human Fc. HeLa cells transfected with an EphA2-Myc expression plasmid were incubated with the crosslinked gH Δ TM-Fc/gL for 1 h at 4 °C, then washed, shifted to 37 °C and fixed with 3% paraformaldehyde after 0 min (top row) or 60 min at 37 °C (second row, enlarged insets in the third row), and analyzed by immunofluorescence. The scale bar in the top left panel is 25 μm and applies to all other images.



EphA2 without the intracellular kinase domain (EphA2 Δ ICMycHis) in 293T cells. We confirmed equal surface expression by FACS analysis (Supplementary Fig. 8). Overexpression of full-length EphA2, but not EphA2 Δ ICMycHis, enhanced KSHV infection in the total cell population by more than 70% (Fig. 3d). We detected a threefold increase in KSHV infection when the analysis was limited to those cells positive for the Myc-tagged EphA2 constructs (Fig. 3d).

To ascertain whether EphA2 is able to mediate uptake of gH Δ TM-Fc/gL, we transiently expressed Myc-tagged EphA2 in HeLa cells. We incubated the cells with cross-linked gH Δ TM-Fc/gL at 4 °C before analyzing the localization of both EphA2 and gH Δ TM-Fc proteins by immunofluorescence. Directly after incubation at 4 °C, EphA2 and gH Δ TM-Fc/gL colocalized at the membrane, whereas after a shift to 37 °C for 60 min both proteins colocalized at vesicular structures within the cell (Fig. 3e). We performed additional experiments to confirm that gH Δ TM-Fc/gL is endocytosed in a fashion analogous to ephrinA1-Fc (Supplementary Fig. 9).

Finally, we examined EphA2 expression in tissue sections from individuals with Kaposi's sarcoma. We stained for the latent KSHV antigen LANA-1 and for EphA2 in consecutive sections of tissues from the skin ($n = 14$) or the lung ($n = 1$) from 15 individuals with AIDS and Kaposi's

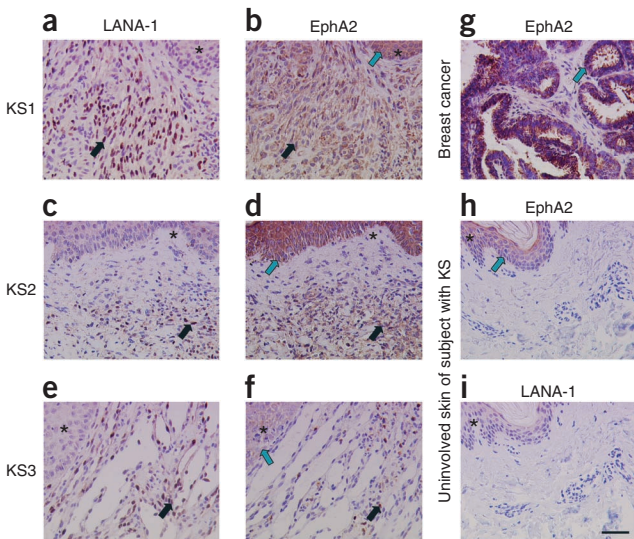


Figure 4 EphA2 and LANA-1 expression in KS. (a–f) Immunohistochemical detection of LANA-1 and EphA2 in two different Kaposi's sarcoma skin lesions (KS1, KS2) and one lung Kaposi's sarcoma (KS3). (g) EphA2 expression in breast cancer, used as a positive control. (h, i) EphA2 and LANA-1 expression in uninvolved tissue sections of the skin of a subject with Kaposi's sarcoma. Similar tissue areas of consecutive sections are indicated by asterisks. Areas with Kaposi's sarcoma spindle cells, showing prominent nuclear LANA-1 staining and cytoplasmic EphA2 staining in consecutive sections, are indicated by black arrows. Teal arrows indicate EphA2 expression in the epidermis overlaying Kaposi's sarcoma (b, d), in the tumor cells of breast cancer (g) or the epidermal layer of uninvolved skin (h). The scale bar in i is 50 μm and applies to all other panels.

sarcoma. In all Kaposi's sarcoma tissues, LANA-1 and EphA2 were expressed in the Kaposi's sarcoma spindle cells (Fig. 4a–f). Kaposi's sarcoma skin tissues showed increased numbers of KSHV-positive cells compared to uninvolved skin from the same individual (Fig. 4a,c), and we detected increased EphA2 staining in the respective consecutive sections (Fig. 4b,d). We also detected numerous KSHV-infected cells in lung Kaposi's sarcoma tissue (Fig. 4e). In lung Kaposi's sarcoma, EphA2 staining resembled the distribution of LANA-1 and both proteins were less homogeneously distributed than in skin Kaposi's sarcoma tissue (Fig. 4f). We used breast carcinoma tissue as a positive control for EphA2 detection (Fig. 4g). Uninvolved skin tissues from the same KS patient stained only slightly positive for EphA2 in the epithelial cells of the epidermis (Fig. 4h) and stained negative for LANA-1 (Fig. 4i). Thus, the percentage of KSHV-infected, LANA-1-positive cells was reflected by the percentage of EphA2-expressing cells. Whereas hardly any EphA2-positive cells were detectable in uninvolved and KSHV-negative skin, the expression of EphA2 was greatly increased in Kaposi's sarcoma specimens from lung and skin, which was paralleled by the number of KSHV-infected cells. In contrast to cells in uninvolved skin, the epidermal cells of the skin overlaying Kaposi's sarcoma tissue were strongly positive for EphA2, suggesting an induction of EphA2 expression in the Kaposi's sarcoma-associated microenvironment (Fig. 4b,d).

This study has shown that EphA2 directly interacts with gH and gL of KSHV. Moreover, interference with this interaction by antibodies against EphA2, by soluble EphA2 ligands, by siRNA-mediated knockdown of EphA2 or by competition with soluble EphA2, but not by closely related Eph proteins, unequivocally inhibited KSHV infection, whereas overexpression of EphA2 enhanced it. Moreover, we showed a strong correlation between EphA2 expression and KSHV infection both in cultured Kaposi's sarcoma-derived cells and in Kaposi's sarcoma tissues (Figs. 2g and 4, respectively). Knockout of both *Epha2* alleles in mice essentially abrogated KSHV infection of mouse endothelial cells (Fig. 2f). Recently, EphA2 was identified as a cellular co-factor for hepatitis C virus (HCV) entry²⁵, organizing other receptors on the cell surface to facilitate virus entry. Thus, the role for EphA2 in the case of HCV infection is mechanistically different, as it seems not to function as a receptor. Still, phosphorylation of EphA2 (Fig. 3a–c) may contribute to KSHV entry by membrane-organizing effects similar to those described for HCV²⁵.

Herpesviral gH-gL proteins mediate entry and fusion, sometimes in a cell-specific manner^{26–30} and in concert with other viral glycoproteins⁴. Unexpectedly, the crystal structures of gH-gL from two herpesviruses, herpes simplex virus and Epstein-Barr virus, did not resemble other viral fusion proteins^{31,32}. KSHV gH-gL has been shown to be required for fusion¹⁶, but further work will be required to define the exact steps of viral entry involving KSHV gH-gL and EphA2. EphA2 ligand binding results in receptor clustering and endocytosis^{33,34}, as does binding of preclustered gH-gL (Fig. 3e and Supplementary Fig. 9). Thus, KSHV mimics ligand-induced activation of EphA2 and may profit from this endocytotic stimulus.

We clearly demonstrate a crucial role of EphA2 in KSHV infection of endothelial cells, the cells from which Kaposi's sarcoma originates³⁵, and show that EphA2 is highly expressed in Kaposi's sarcoma tissue sections (Fig. 4a–f). EphA2, EphA4 and EphB2 are known to be phosphorylated in Kaposi's sarcoma tissues^{36,37}, and EphA2 activation is an important factor in angiogenesis^{36,38}. In turn, Kaposi's sarcoma is an angiogenic tumor characterized by chronic, ongoing KSHV infection and neovascularization. The known proangiogenic properties of EphA2 together with the findings of this study support the hypothesis that KSHV interaction with EphA2 is implicated in Kaposi's sarcoma pathogenesis.

Therapeutic synergies between inhibiting viral entry and blocking angiogenesis by targeting EphA2 may be beneficial in the treatment of this disease.

METHODS

Methods and any associated references are available in the online version of the paper.

Note: Supplementary information is available in the online version of the paper.

ACKNOWLEDGMENTS

This work was supported by the Akademie der Wissenschaften und der Literatur (Mainz), the European Community research project TargetHerpes, Deutsche Forschungsgemeinschaft center grant 643 and graduate school grant 1071 "viruses of the immune system." M. Stürzl, E.N. and F.N. were supported by the interdisciplinary center for clinical research at the University Hospital of the University of Erlangen. M. Stürzl and E.N. were supported by the German Cancer Aid. We thank L. Wall for experimental assistance and R.C. Desrosiers for helpful discussions and critical reading of the manuscript. K562 cells were kindly provided by A. Albin (Science and Technology Pole, IRCCS MultiMedica). 4G10 mouse hybridoma supernatant was kindly provided by B. Biesinger (Virologisches Institut, Universitätsklinikum Erlangen).

AUTHOR CONTRIBUTIONS

A.S.H. and F.N. designed the study. A.S.H., J.K.K. and E.W. performed the key experiments. J.P.-I., K.S., M. Schmidt and A.H. performed real-time PCR experiments, cell culture and infection assays. S.K. performed mass spectrometry and analyzed the data. J.C., A.E., J.M. and N.H.B. contributed key reagents. E.N. and M. Stürzl helped with endothelial cell cultures and performed immunohistochemistry experiments. A.S.H. and F.N. wrote the manuscript. B.F. contributed expertise and helped write the paper.

COMPETING FINANCIAL INTERESTS

The authors declare competing financial interests: details are available in the online version of the paper.

Published online at <http://www.nature.com/doi/10.1038/nm.2805>.

Reprints and permissions information is available online at <http://www.nature.com/reprints/index.html>.

- Chang, Y. *et al.* Identification of herpesvirus-like DNA sequences in AIDS-associated Kaposi's sarcoma. *Science* **266**, 1865–1869 (1994).
- Cesarman, E., Chang, Y., Moore, P.S., Said, J.W. & Knowles, D.M. Kaposi's sarcoma-associated herpesvirus-like DNA sequences in AIDS-related body-cavity-based lymphomas. *N. Engl. J. Med.* **332**, 1186–1191 (1995).
- Soulier, J. *et al.* Kaposi's sarcoma-associated herpesvirus-like DNA sequences in multicentric Castlemann's disease. *Blood* **86**, 1276–1280 (1995).
- Campadelli-Fiume, G. *et al.* The multipartite system that mediates entry of herpes simplex virus into the cell. *Rev. Med. Virol.* **17**, 313–326 (2007).
- Akula, S.M. *et al.* Kaposi's sarcoma-associated herpesvirus (human herpesvirus 8) infection of human fibroblast cells occurs through endocytosis. *J. Virol.* **77**, 7978–7990 (2003).
- Raghu, H., Sharma-Walia, N., Veetil, M.V., Sadagopan, S. & Chandran, B. Kaposi's sarcoma-associated herpesvirus utilizes an actin polymerization-dependent macropinocytic pathway to enter human dermal microvascular endothelial and human umbilical vein endothelial cells. *J. Virol.* **83**, 4895–4911 (2009).
- Chandran, B. Early events in Kaposi's sarcoma-associated herpesvirus infection of target cells. *J. Virol.* **84**, 2188–2199 (2010).
- Birkmann, A. *et al.* Cell surface heparan sulfate is a receptor for human herpesvirus 8 and interacts with envelope glycoprotein K8.1. *J. Virol.* **75**, 11583–11593 (2001).
- Wang, F.Z., Akula, S.M., Pramod, N.P., Zeng, L. & Chandran, B. Human herpesvirus 8 envelope glycoprotein K8.1A interaction with the target cells involves heparan sulfate. *J. Virol.* **75**, 7517–7527 (2001).
- Akula, S.M., Pramod, N.P., Wang, F.Z. & Chandran, B. Human herpesvirus 8 envelope-associated glycoprotein B interacts with heparan sulfate-like moieties. *Virology* **284**, 235–249 (2001).
- Hahn, A. *et al.* Kaposi's sarcoma-associated herpesvirus gH/gL: Glycoprotein export and interaction with cellular receptors. *J. Virol.* **83**, 396–407 (2009).
- Rappocciolo, G. *et al.* DC-SIGN is a receptor for human herpesvirus 8 on dendritic cells and macrophages. *J. Immunol.* **176**, 1741–1749 (2006).
- Sharma-Walia, N., Naranatt, P.P., Krishnan, H.H., Zeng, L. & Chandran, B. Kaposi's sarcoma-associated herpesvirus/human herpesvirus 8 envelope glycoprotein gB induces the integrin-dependent focal adhesion kinase-Src-phosphatidylinositol 3-kinase-Rho GTPase signal pathways and cytoskeletal rearrangements. *J. Virol.* **78**, 4207–4223 (2004).

14. Naranatt, P.P., Akula, S.M., Zien, C.A., Krishnan, H.H. & Chandran, B. Kaposi's sarcoma-associated herpesvirus induces the phosphatidylinositol 3-kinase-PKC- ζ -MEK-ERK signaling pathway in target cells early during infection: implications for infectivity. *J. Virol.* **77**, 1524–1539 (2003).
15. Kaleeba, J.A.R. & Berger, E.A. Kaposi's sarcoma-associated herpesvirus fusion-entry receptor: cystine transporter xCT. *Science* **311**, 1921–1924 (2006).
16. Pertel, P.E. Human herpesvirus 8 glycoprotein B (gB), gH, and gL can mediate cell fusion. *J. Virol.* **76**, 4390–4400 (2002).
17. Banfield, B.W., Leduc, Y., Esford, L., Schubert, K. & Tufaro, F. Sequential isolation of proteoglycan synthesis mutants by using herpes simplex virus as a selective agent: evidence for a proteoglycan-independent virus entry pathway. *J. Virol.* **69**, 3290–3298 (1995).
18. Zhu, L., Puri, V. & Chandran, B. Characterization of human herpesvirus-8 K8.1A/B glycoproteins by monoclonal antibodies. *Virology* **262**, 237–249 (1999).
19. Brantley-Sieders, D.M. *et al.* EphA2 receptor tyrosine kinase regulates endothelial cell migration and vascular assembly through phosphoinositide 3-kinase-mediated Rac1 GTPase activation. *J. Cell Sci.* **117**, 2037–2049 (2004).
20. Vieira, J. & O'Hearn, P.M. Use of the red fluorescent protein as a marker of Kaposi's sarcoma-associated herpesvirus lytic gene expression. *Virology* **325**, 225–240 (2004).
21. Stürzl, M. *et al.* Identification of interleukin-1 and platelet-derived growth factor-B as major mitogens for the spindle cells of Kaposi's sarcoma: a combined *in vitro* and *in vivo* analysis. *Oncogene* **10**, 2007–2016 (1995).
22. Albin, A. *et al.* The beta-core fragment of human chorionic gonadotrophin inhibits growth of Kaposi's sarcoma-derived cells and a new immortalized Kaposi's sarcoma cell line. *AIDS* **11**, 713–721 (1997).
23. Herndier, B.G. *et al.* Characterization of a human Kaposi's sarcoma cell line that induces angiogenic tumors in animals. *AIDS* **8**, 575–581 (1994).
24. Kaleeba, J.A.R. & Berger, E.A. Broad target cell selectivity of Kaposi's sarcoma-associated herpesvirus glycoprotein-mediated cell fusion and virion entry. *Virology* **354**, 7–14 (2006).
25. Lupberger, J. *et al.* EGFR and EphA2 are host factors for hepatitis C virus entry and possible targets for antiviral therapy. *Nat. Med.* **17**, 589–595 (2011).
26. Vleck, S.E. *et al.* Structure–function analysis of varicella-zoster virus glycoprotein H identifies domain-specific roles for fusion and skin tropism. *Proc. Natl. Acad. Sci. USA* **108**, 18412–18417 (2011).
27. Chesnokova, L.S., Nishimura, S.L. & Hutt-Fletcher, L.M. Fusion of epithelial cells by Epstein-Barr virus proteins is triggered by binding of viral glycoproteins gHgL to integrins $\alpha_5\beta_1$ or $\alpha_5\beta_3$. *Proc. Natl. Acad. Sci. USA* **106**, 20464–20469 (2009).
28. Chesnokova, L.S. & Hutt-Fletcher, L.M. Fusion of EBV with epithelial cells can be triggered by $\alpha_5\beta_1$ in addition to $\alpha_5\beta_3$ and $\alpha_5\beta_3$ and integrin binding triggers a conformational change in gHgL. *J. Virol.* **85**, 13214–13223 (2011).
29. Vanarsdall, A.L., Chase, M.C. & Johnson, D.C. Human cytomegalovirus glycoprotein gO complexes with gH-gL, promoting interference with viral entry into human fibroblasts but not entry into epithelial cells. *J. Virol.* **85**, 11638–11645 (2011).
30. Ryckman, B.J., Chase, M.C. & Johnson, D.C. HCMV gH/gL/UL128–131 interferes with virus entry into epithelial cells: evidence for cell type-specific receptors. *Proc. Natl. Acad. Sci. USA* **105**, 14118–14123 (2008).
31. Chowdary, T.K. *et al.* Crystal structure of the conserved herpesvirus fusion regulator complex gH-gL. *Nat. Struct. Mol. Biol.* **17**, 882–888 (2010).
32. Matsuura, H., Kirschner, A.N., Longnecker, R. & Jaretzky, T.S. Crystal structure of the Epstein-Barr virus (EBV) glycoprotein H/glycoprotein L (gH/gL) complex. *Proc. Natl. Acad. Sci. USA* **107**, 22641–22646 (2010).
33. Walker-Daniels, J., Riese, D.J. & Kinch, M.S. c-Cbl-dependent EphA2 protein degradation is induced by ligand binding. *Mol. Cancer Res.* **1**, 79–87 (2002).
34. Zhuang, G., Hunter, S., Hwang, Y. & Chen, J. Regulation of EphA2 receptor endocytosis by SHIP2 lipid phosphatase via phosphatidylinositol 3-kinase-dependent Rac1 activation. *J. Biol. Chem.* **282**, 2683–2694 (2007).
35. Wang, H.W. *et al.* Kaposi sarcoma herpesvirus-induced cellular reprogramming contributes to the lymphatic endothelial gene expression in Kaposi sarcoma. *Nat. Genet.* **36**, 687–693 (2004).
36. Ogawa, K. *et al.* The ephrin-A1 ligand and its receptor, EphA2, are expressed during tumor neovascularization. *Oncogene* **19**, 6043–6052 (2000).
37. Scheinet, J.S. *et al.* The role of Ephs, ephrins and growth factors in Kaposi sarcoma and implications of ephrinB2 blockade. *Blood* **113**, 254–263 (2009).
38. Cheng, N. *et al.* Blockade of EphA receptor tyrosine kinase activation inhibits vascular endothelial cell growth factor-induced angiogenesis. *Mol. Cancer Res.* **1**, 2–11 (2002).

ONLINE METHODS

Cells, virus, plasmids, transfection and recombinant protein production.

Adherent cell lines were cultivated in DMEM supplemented with 10% FBS and gentamycin at 37 °C, 7% CO₂ at 80% humidity. Human LECs and mouse³⁹ endothelial cells were cultivated in EGM-2 MV (Lonza). Lung microvascular endothelial cells were isolated from WT and *Epha2*-knockout mice as described before³⁹. Transduction with LZRS retrovirus expressing WT EphA2 has been described earlier³⁹. All mice were housed under pathogen-free conditions, and experiments were performed in accordance with the Association and Accreditation of Laboratory Animal Care International guidelines and with approval by the Vanderbilt University Institutional Animal Care and Use Committee. Human LECs were purchased from Lonza. HUVECs were purchased from Promocell and maintained in endothelial cell growth medium (Promocell). KSIImm cells were kindly provided by A. Albini. SLK⁴⁰ cells were obtained from the US National Institutes of Health AIDS Research and Reference Reagent program (catalog no. 9402). RD⁴¹ and HepG2 (ref. 42) cells were obtained from American Type Culture Collection. M7/2 Kaposi's sarcoma cells have been described before⁴³. rKSHV.219⁴⁴ virus preparation and infection assays were carried out essentially as described previously⁴⁵. Tangential flow filtration followed by diafiltration against PBS was used as the first step to concentrate and purify KSHV virions from the supernatant of lytically induced cells in a protocol modified from reference 46. Briefly, the mini-mate system (PALL Life Sciences) and tangential flow filtration capsules with a cutoff of 300 kDa were used according to the manufacturer's instructions. A transmembrane pressure of 1 bar was used at a flow rate of 80 ml min⁻¹. Further virus purification was performed by centrifugation on Opti-Prep (iodixanol) gradients⁴⁷. For KSHV infections at low titer, supernatant from rKSHV.219-producing 293 cells was concentrated by centrifugation as previously described⁴⁸. Unless stated otherwise, KSHV was used at a multiplicity of infection of 0.5 as determined on SLK cells. For infection of MPMECs, an SLK multiplicity of infection of 2 was used. A recombinant, GFP-expressing clone of herpesvirus saimiri (HVS-M45) was generated by recombination of five overlapping cosmids⁴⁹. Here, the HVS oncogenes *stpC* and *tip* were deleted by digestion of cosmid 331EGFP (ref. 50) with Bst1107I, followed by religation, yielding cosmid 331EGFP-Δ*StpC/Tip*. Blocking of infection with soluble receptor was assayed by a 30-min preincubation of the virus dilution at room temperature with EphA2-Fc or Fc at 2 μg ml⁻¹ if not indicated otherwise and subsequent infection. Recombinant Fc-fusion proteins were prepared as described previously⁵¹. Strep-tagged versions of gHATM-Fc and Fc were purified under native conditions by StrepTactin chromatography and elution with 3 mM biotin in PBS. Soluble EphA2-Fc comprises amino acids 25–534 of human EphA2 in the pAB61 Fc-fusion backbone vector. Soluble EphA2-HA comprises amino acids 1–534 fused to the hemagglutinin epitope in the pcDNA6 backbone. EphrinA1-Fc comprises amino acids 19–188 of human ephrinA1 (EFNA1) in the pAB61 Fc-fusion backbone vector. Expression plasmid pEphA2MycHis (full length, ref[NP_004422.2]) was generated by PCR amplification of the respective fragment from EphA2 cDNA. The resulting amplicon was inserted into the pcDNA4a backbone. An antiserum against EphA2 was raised in rabbits using recombinant soluble EphA2. Whole antibodies were purified from this serum using protein A-Sepharose. For blocking purposes, polyclonal antibody was used at 1 mg ml⁻¹.

Transfection was carried out as described previously⁴⁸. Stably transfected cell populations were generated by selection with 100 μg ml⁻¹ Zeocin (Invitrogen). Octyl-β-D-glucopyranoside formulations of human integrins α₃β₁ (catalog no. CC1029) and α_vβ₃ (cat. no. CC1020) were purchased from Upstate Biotechnology/Millipore. EphA2-specific monoclonal antibody D7 (catalog no. 05-480, dilution 1:500) and integrin α_vβ₃-specific antibody clone LM609 (catalog no. MAB1976, used at 10 μg/ml) were purchased from Chemicon/Millipore. Recombinant human EphA2, EphA5 and ephrinA4-Fc were purchased from R&D; recombinant EphA4 was purchased from Biomol.

Surface biotinylation, immunoprecipitation and mass spectrometry.

Biotinylation of cellular membrane proteins was performed with EZ-link Sulfo-NHS-Biotin (Pierce) according to the manufacturer's instructions. For immunoprecipitation, cells were lysed in 1% NP-40, 150 mM NaCl, 2.5 mM EDTA/EGTA, 20 mM HEPES pH 7.4. The lysates were cleared by centrifugation

at 20,000g, and supernatants were immunoprecipitated with Fc-fusion proteins coupled to protein A-Sepharose (GE Healthcare). Coupling of proteins was achieved by preadsorbing 1 ml of protein containing supernatant per sample to the protein A-Sepharose beads. For mass-spectrometry analysis, three densely confluent 10-cm culture dishes of sog9 mouse fibroblasts were used per immunoprecipitation sample. For small-scale immunoprecipitation, approximately two million transfected 293T cells were lysed. Samples were washed three times with lysis buffer, separated on 8–16% PAA gradient gels (Invitrogen) and stained with colloidal Coomassie blue or subjected to western blot analysis. Bands were excised from the gel and prepared for mass-spectrometric identification as described earlier⁵². Briefly, the protein was digested in the gel using trypsin. The peptides were extracted and desalted for MALDI-TOF mass spectrometry (MALDI Micro MX; Waters). In addition, the extract was applied to nanoLC-MS/MS using UPLC and Q-TOF Premier (Waters). Both methods independently identified EphA2 (**Supplementary Table 1**).

For co-sedimentation of KSHV with EphA2, BC3 cells were induced with 3 mM sodium butyrate to produce virus or left uninduced. Supernatants were precleared for 10 min at 3,000g and then centrifuged for 6 h at 5,000g. Supernatant was aspirated down to one-tenth of the original volume. Soluble EphA2-HA was expressed in 293T cells. Supernatant of EphA2-HA-expressing cells was precleared by centrifugation at 16,000g for 10 min. Equal amounts of BC3 and supernatant from EphA2-HA-expressing cells were mixed and incubated for 2 h at room temperature, precleared for 5 min at 3,000g and pelleted for 2 h at 16,000g. The pellet was washed twice with PBS and re-pelleted for 30 min at 16,000g, followed by western blot analysis.

FACS binding assays. Protein-containing supernatants from transfected 293T cells were assayed by western blotting for comparable protein expression levels. Further purification was omitted in order to not damage the noncovalent gH-gL interaction. These supernatants were buffered by addition of HEPES at a final concentration of 25 mM and used for binding studies, which were carried out as described previously⁴⁸. Cells were incubated with the protein-containing supernatants for 1 h, washed and then incubated with FITC-conjugated antibody to human Fc (Dako, F0202) at a dilution of 1:100 for 1 h, washed again and analyzed on a Becton-Dickinson FACSCalibur. All steps were performed at 4 °C or on ice. For competition of gHTM-FcStrep/gL binding to cell surfaces by soluble receptor, gHTM-FcStrep/gL-containing supernatants were preincubated for 30 min at room temperature with EphA2-Fc or Fc at the concentrations indicated in **Figure 1f**. The binding assays themselves were carried out as described above except that StrepTactin-phycoerythrin (IBA) was used for secondary detection.

siRNA transfection. LECs were seeded in 12-well plates and transfected at ~70% confluency with siRNA pools from Dharmacon targeting either EphA2 (siGENOME SMARTpool siRNA D-003116-06) or EphB4 (siGENOME SMARTpool M-003124-02-0005) or nontargeting siRNA pool (siGENOME Non-Targeting siRNA Pool #2 D-001206-14-05). For one well, 50 nmol of each pool were diluted in 25 μl H₂O and 25 μl OptiMEM (Gibco). One microliter of Dharmafect-1 (Dharmacon) prediluted in 50 μl OptiMEM was added followed by mixing and 5 min of incubation. Four hundred microliters of EGM-2 MV growth medium were added, and the whole mixture was applied to the cells. Medium was exchanged after 24 h.

RNA extraction and quantitative reverse-transcription PCR. Total cellular RNA was extracted from cultured cells using the Nucleospin RNA II kit (Machery&Nagel) according to the manufacturer's instructions. Simultaneous quantitative reverse-transcription PCR for KSHV LANA-1 and GAPDH transcripts was performed using the Quantitect Multiplex RT-PCR kit (Qiagen) according to the manufacturer's instructions. Oligonucleotides qRT-LANA-Fw (5'-TCC GGC TGA CTT ATA AAC AAC CAG ATT TC-3'), qRT-LANA-Rev (5'-TCC GCA CCT CAG GCG CA-3'), qRT-GAPDH-Fw (5'-GCC TCA AGA TCA TCA GCA ATG CC-3'), qRT-GAPDH-Rev (5'-CCA CGA TCA CAA AGT TGT CAT GGA-3') and labeled probes for LANA-1 (5'-FAM-CGA GGA TGG CGC CCC CGG GA -BHQ-1-3') and GAPDH (5'-Yakima-Yellow-CCT GCA CCA CCA ACT GCT TAG CAC C -BHQ-1-3') were used for the simultaneous detection of LANA-1 and GAPDH transcripts. PCR efficiency

was determined and used to calculate relative transcript levels using the $\Delta\Delta C_t$ method. Quantification of EphA2 and actin transcripts was done with a two-step RT-PCR and SYBR-green labeling as described before (oligonucleotides: EphA2-RT-1830-Fw: 5'-ATC CTG TGT CAC TCG GCA GAA G-3'; EphA2-RT-2038-Rev: 5'-CCT CTA GGC GGA TGA TGT TGT G-3'; Aktin-Fw: 5'-CCA TCT ACG AGG GGT ATG-3'; Aktin-Rev: 5'-CGT GGC CAT CTC TTG CTC-3')⁵³. Absolute quantification was done using a standard curve obtained from diluted plasmid DNA.

Detection of EphA2 phosphorylation. EphA2 phosphorylation in 293T cells was measured with DuoSet IC Human Phospho-EphA2 ELISA (R&D Systems). Stimulation was achieved by inoculating the cells for 10 min with rKSHV.219 (ten genome copies per cell) or an identically prepared control preparation from the supernatant of chemically induced KSHV-negative 293 cells. Alternatively, 293T cells were stimulated with either rKSHV.219, cell culture medium or purified proteins and lysed in 1% NP-40, 150 mM NaCl, 2.5 mM EDTA/EGTA, 20 mM HEPES pH 7.4 with addition of 5 mM sodium orthovanadate and 1 mM PMSF. Intrinsic EphA2 was precipitated with protein A-Sepharose preadsorbed with 50 μ l of anti-EphA2 rabbit serum (Primm, rabbit immunized with EphA2-Fc). For precipitation of Myc-tagged recombinant EphA2, antibody 9E10 (American Type Culture Collection, CRL-1729) directed against the Myc epitope coupled to protein A-Sepharose was used. Immunoprecipitation was followed by western blotting against phosphotyrosine (4G10 mouse hybridoma supernatant, a kind gift from B. Biesinger) and EphA2 (Sigma, anti-EphA2 6F8 from mouse, dilution 1:1,000).

Immunofluorescence and endocytosis assay. gHTM-FcStrep/gL, ephrinA1-Fc or Fc proteins were preincubated for 30 min at room temperature with anti-human-Fc secondary antibodies (1:100) indicated in **Figure 3c** for cross-linking. The proteins were then incubated with cells on cover slips for 1 h at 4 °C. After a brief wash, the cells were shifted to 37 °C and subjected to immunofluorescence analysis at the time points indicated in the legend to **Figure 3c**. The cells were briefly rinsed with PBS three times and fixed with 3% paraformaldehyde in PBS, followed by quenching with 0.1 M glycine and permeabilization with 0.1% NP-40 in PBS for 5 min. After blocking with 2% BSA and 5% FBS in PBS, the cells were incubated with the respective antibodies where indicated for 1 h at room temperature and mounted with ProLong Gold mounting medium (Invitrogen). Images were acquired on a Leica TCS SP5 confocal laser scanning microscope in sequential scanning mode to eliminate crosstalk.

Immunohistochemistry. Kaposi's sarcoma tissues were obtained from 15 HIV-1-infected individuals with AIDS in the context of medically required diagnostic or therapeutic procedures. Informed consent was obtained from all subjects (skin KS, $n = 14$; lung KS, $n = 1$). Staining of paraformaldehyde-fixed, paraffin-embedded tissue sections for EphA2 and LANA-1 were performed as previously described⁵⁴. A rabbit polyclonal antibody directed against human EphA2 (Santa Cruz, sc-924, diluted 1:100) and a rat monoclonal antibody against LANA-1 (Tebu-bio, catalog no. 13-210-100, diluted 1:250) were used as primary antibodies. Primary antibody binding was detected using the respective

Vectastain Elite ABC Kits (Vector Laboratories). For both antibodies, the citrate buffer pH 6.0 (DakoCytomation) was used for the antigen retrieval. The sections were then developed using NovaRed Substrate (Vector Laboratories) and counterstained with Hematoxylin Gill III (Merck, Darmstadt, Germany). Stained cells were photographed using an Aristoplan microscope (Leica, Wetzlar, Germany) equipped with 10 \times and 25 \times objectives and a 3CCD Exwave HAD color camera (Sony, Berlin, Germany). Control staining was performed without primary antibody and yielded negative results (data not shown).

Statistical analyses. All results are expressed as arithmetic means. Error bars represent either s.e.m or s.d. Data were analyzed with unpaired two-tailed *t* tests (SPSS 16, GraphPad Prism 5).

39. Brantley-Sieders, D.M. *et al.* EphA2 receptor tyrosine kinase regulates endothelial cell migration and vascular assembly through phosphoinositide 3-kinase-mediated Rac1 GTPase activation. *J. Cell Sci.* **117**, 2037–2049 (2004).
40. Herndier, B.G. *et al.* Characterization of a human Kaposi's sarcoma cell line that induces angiogenic tumors in animals. *AIDS* **8**, 575–581 (1994).
41. McAllister, R.M., Melnyk, J., Finkelstein, J.Z., Adams, E.C. Jr. & Gardner, M.B. Cultivation *in vitro* of cells derived from a human rhabdomyosarcoma. *Cancer* **24**, 520–526 (1969).
42. Knowles, B.B., Howe, C.C. & Aden, D.P. Human hepatocellular carcinoma cell lines secrete the major plasma proteins and hepatitis B surface antigen. *Science* **209**, 497–499 (1980).
43. Stürzl, M. *et al.* Identification of interleukin-1 and platelet-derived growth factor-B as major mitogens for the spindle cells of Kaposi's sarcoma: a combined *in vitro* and *in vivo* analysis. *Oncogene* **10**, 2007–2016 (1995).
44. Vieira, J. & O'Hearn, P.M. Use of the red fluorescent protein as a marker of Kaposi's sarcoma-associated herpesvirus lytic gene expression. *Virology* **325**, 225–240 (2004).
45. Myoung, J. & Ganem, D. Generation of a doxycycline-inducible KSHV producer cell line of endothelial origin: Maintenance of tight latency with efficient reactivation upon induction. *J. Virol. Methods* **174**, 12–21 (2011).
46. Wickramasinghe, S.R., Kalbfuss, B., Zimmermann, A., Thom, V. & Reichl, U. Tangential flow microfiltration and ultrafiltration for human influenza A virus concentration and purification. *Biotechnol. Bioeng.* **92**, 199–208 (2005).
47. Garrigues, H.J., Rubinchikova, Y.E., DiPersio, C.M. & Rose, T.M. Integrin $\alpha_v\beta_3$ Binds to the RGD motif of glycoprotein B of Kaposi's sarcoma-associated herpesvirus and functions as an RGD-dependent entry receptor. *J. Virol.* **82**, 1570–1580 (2008).
48. Hahn, A. *et al.* Kaposi's sarcoma-associated herpesvirus gH-gL: glycoprotein export and interaction with cellular receptors. *J. Virol.* **83**, 396–407 (2009).
49. Ensser, A., Pfänder, A., Müller-Fleckenstein, I. & Fleckenstein, B. The URNA genes of herpesvirus saimiri (strain C488) are dispensable for transformation of human T cells *in vitro*. *J. Virol.* **73**, 10551–10555 (1999).
50. Glykofrydes, D. *et al.* Herpesvirus saimiri vFLIP provides an antiapoptotic function but is not essential for viral replication, transformation, or pathogenicity. *J. Virol.* **74**, 11919–11927 (2000).
51. Birkmann, A. *et al.* Cell surface heparan sulfate is a receptor for human herpesvirus 8 and interacts with envelope glycoprotein K8.1. *J. Virol.* **75**, 11583–11593 (2001).
52. König, S. *et al.* Sodium dodecyl sulfate versus acid-labile surfactant gel electrophoresis: comparative proteomic studies on rat retina and mouse brain. *Electrophoresis* **24**, 751–756 (2003).
53. Schmidt, K., Wies, E. & Neipel, F. Kaposi's sarcoma-associated herpesvirus viral interferon regulatory factor 3 inhibits gamma interferon and major histocompatibility complex class II expression. *J. Virol.* **85**, 4530–4537 (2011).
54. Naschberger, E. *et al.* Angiostatic immune reaction in colorectal carcinoma: impact on survival and perspectives for antiangiogenic therapy. *Int. J. Cancer* **123**, 2120–2129 (2008).